Geophysical Research Letters

RESEARCH LETTER
10.1029/2019GL084302

The Role of the Amazon River Plume on the Intensification of the Hydrological Cycle

N. A. Gouveia[1], D. F. M. Gherardi[1], and L. E. O. C. Aragão[1]

[1]Remote Sensing Division National Institute for Space Research- INPE, São José dos Campos, Brazil

Key Points:
- The positive trend in water storage over the western Amazon has reduced the salinity of the Amazon River plume spreading to the Atlantic
- Surface salinity in the main export pathway of the Amazon River plume responds to the hydrological cycle intensification
- The hydrological intensification increases the eastward export of the Amazon plume water

Supporting Information:
- Supporting Information S1

Correspondence to:
N. A. Gouveia,
nelson.gouveia@inpe.br

Citation:
Gouveia, N. A., Gherardi, D. F. M., & Aragão, L. E. O. C. (2019). The role of the Amazon River plume on the intensification of the hydrological cycle. *Geophysical Research Letters*, *46*, 12,221–12,229. https://doi.org/10.1029/2019GL084302

Received 28 JUN 2019
Accepted 26 OCT 2019
Published online 12 NOV 2019

Abstract The Amazon River low-salinity plume takes part in important ocean and atmosphere processes that influence climate. In the last three decades, the intensification of the hydrological cycle has increased the interannual variability of total freshwater discharged into the ocean. However, the feedback mechanisms of the Amazon River plume acting on this intensification are not fully understood. Correlation maps and multiple regression analysis applied to 16 years of satellite data and river flow measurements indicate that a positive precipitation trend of 15 mm/year in the western Amazon basin follows the long-term warming of the tropical Atlantic. This increased the total amount of freshwater discharged into the ocean and reduced the Amazon River plume salinity by 3.5% per year in the main plume water export pathway. Based on these results we propose a process-oriented model of the feedback process that explains the intensification of the Amazon hydrological cycle.

Plain Language Summary Since 2009 the Amazon Basin has experienced increasing river flows during the wet season and reduced water levels during the dry season. This has been called by experts as the intensification of the hydrological cycle. This phenomenon has already been observed before and it can affect the surface salinity of the tropical Atlantic. We are taking advantage of this process to identify what part of the Amazon River basin contributes most to the reduction of surface salinity in the tropical Atlantic and its possible feedback mechanism to the climate system. The analysis of different satellite data and in situ measurements allowed us to determine that the vertically accumulated water on the western portion of the Amazon River basin is responsible for most of the change in surface salinity of the tropical Atlantic Ocean. We also propose a conceptual model to explain how the ocean, the atmosphere, and the Amazon forest interact to cause this hydrological intensification.

1. Introduction

The Amazon basin carries annually 6.6×10^3 km^3 of freshwater into the western tropical North Atlantic (WTNA) Ocean, representing about 50% of the total continental water inflow to the Atlantic Ocean (Dai & Trenberth, 2002; Korosov et al., 2015; Salisbury et al., 2011). The Amazon River plume (ARp) is transported up to 1,000 km away from the coast in four main water export pathways (Coles et al., 2013; Masson & Delecluse, 2001). Amazon discharge peaks in spring (April–May) during the northward migration of the intertropical convergence zone (ITCZ) when onshore winds are relaxed. In the following summer (June–July) river discharge starts feeding the North Equatorial Counter Current (NECC) and in September 70% of ARp water is exported eastward by this pathway (Lentz & Limeburner, 1995). The ARp water also influences a number of important process such as carbon sequestration from primary production (Gouveia et al., 2019; Medeiros et al., 2015; Stukel et al., 2014; Subramaniam et al., 2008), heat flux (Field, 2007; Foltz & McPhaden, 2008), barrier layer formation (Balaguru et al., 2012; Pailler et al., 1999), and ocean circulation (Coles et al., 2013). Variations in the Amazon River discharge is a key driver of ARp changes (Hu et al., 2004; Muller-Karger et al., 1988; Salisbury et al., 2011; Zeng et al., 2008). Zeng et al. (2008) analyzed the interannual variability of ARp and found a positive correlation between the river discharge anomalies at Óbidos station and anomalies of the ARp extent ($r = 0.58$). The northwestward export of plume water to the Caribbean by the Guiana Current can be also influenced by weak onshore winds and eddy-shelf interactions (Fournier et al., 2017).

The Amazon River runoff responds to the variability and intensity of precipitation over the Amazon River basin (ARB). The Tropical Atlantic Ocean and the recycled continental moisture are the main sources of water for precipitation (Drumond et al., 2014; Eltahir & Bras, 1994; Enfield, 1996; Marengo, 2006). The

former influences the northern ARB portion, whereas the latter depends on the evapotranspiration (Sorí et al., 2018). The northwest of the ARB concentrates the highest precipitation rates of the basin (> 2,500 mm average per year) (Espinoza et al., 2009; Espinoza et al., 2015), influenced by the seasonal displacement of the ITCZ and the meridional sea surface temperature (SST) gradient of tropical Atlantic (Xie & Carton, 2004). In addition, the balance between precipitation and evapotranspiration of the ARB indicates a moisture sink in the region with precipitation generally overcoming evapotranspiration (Nascimento et al., 2016; Marengo, 2005).

The ARB hydrological cycle is intensifying in the last three decades, with extreme floods and droughts associated with ocean evaporation that modulates continental precipitation (Espinoza et al., 2014; Gloor et al., 2013; Marengo et al., 2008; Marengo et al., 2011). This moisture transport from ocean to land directly impacts the total water discharged into the WTNA and the sea surface salinity (SSS). It has been shown that SSS can be used as an indicator of moisture flux divergence over the ocean and convergence over land in the subtropical North Atlantic (Li et al., 2016). This study aims to identify covariation patterns between hydrological components of ARB and the main water export pathway through the NECC. We also assess the possible feedback mechanisms behind the Amazon hydrological cycle intensification that include precipitation over the ARB, the SSS of the NECC (SSS_{NECC}), and the export of ARp water and SST anomalies (SSTAs) on the tropical Atlantic and the Pacific.

2. Materials and Methods

2.1. Data and Methodology

The study area comprises the ARB and WTNA, with a focus on the river water export pathway through the NECC (Figure 1). The NECC is the main export of low-salinity water to the interior of the subtropical gyre and the NECC jet (Coles et al., 2013) and is characterized by sharp SSS_{NECC} gradients. The monthly data sets span from July 2002 to August 2017 and the ARB hydrological variables are (i) precipitation data from the Tropical Rainfall Measuring Mission (TRMM) satellite of the TRMM 3B43v7 product with 0.25° spatial resolution available at https://disc.gsfc.nasa.gov/datasets/TRMM_3B43V7/summary (Huffman et al., 2007; Huffman et al., 2010); (ii) total water storage (TWS) from the Gravity Recovery and Climate Experiment with 1° spatial resolution RL05 from the German Research Centre for Geoscience available at http://grace.jpl.nasa.gov/data/get-data/ (Dahle et al., 2012); (iii) river discharge from 16 in situ flow stations, located along the main rivers and representing the runoff of all Amazon sub-basins (Madeira, Solimões, Xingu, Negro, and Tapajós) (Figure 1) obtained from the Hydrogeodynamics of the Amazon Basin Observatory (ORE-HYBAM) (http://www.ore-hybam.org/); and (iv) monthly average SSS_{NECC} (black box in Figure 1) estimated using Moderate Resolution Imaging Spectroradiometer (MODIS) products following Gouveia et al. (2019), see Text S1 in the supporting information for details). We chose the NECC pathway (Figure 1) because it transports up to 70% of the Amazon plume water that is deflected eastward by the North Brazil Current (NBC) retroflection (Grodsky et al., 2014; Lentz & Limeburner, 1995). We used the ARP maximum salinity threshold of 35 practical salinity units (psu) computed for the black rectangle area in Figure 1 to calculate the maximum monthly eastward extension of the plume. The Atlantic Multidecadal Oscillation, the North Tropical Atlantic (NTA, https://www.esrl.noaa.gov/psd/data/climateindices/list/), and the El Niño Modoki (ENM, Text S2) (http://www.jamstec.go.jp/frsgc/research/d1/iod/DATA/emi.monthly.txt) were used as proxy climate indicators for SSS_{NECC} variability (Figure 1).

Correlations were calculated for every pixel within the ARB between seasonal standardized anomalies of precipitation, TWS, river runoff at each measuring station, overall years, and SSS_{NECC} (monthly mean of SSS calculated for the NECC area inside the black rectangle) (Figure 1) anomalies to assess the possible links between ARB hydrology and the eastward export of plume water in the tropical Atlantic. The wet season was defined from November to April, and the dry season from June to October, following Gloor et al. (2015). The SSS_{NECC} anomalies were calculated for the area 1 where the ARP is found within the NECC. Trend regression slopes were tested with Student's t test with a 5% significance level, and a seasonal trend decomposition was computed based on a nonparametric local regression Locally Estimated Scatterplot Smoothing (LOESS), Cleveland et al. (1990).

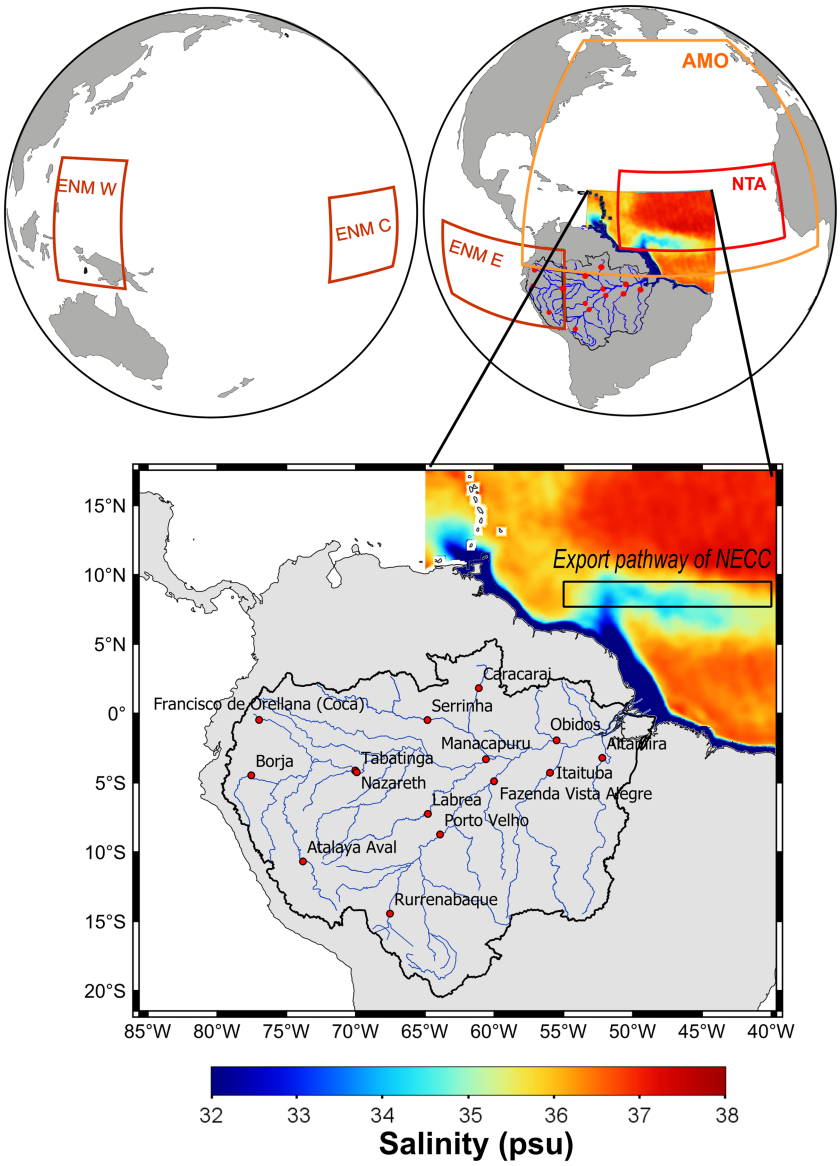

Figure 1. Study area comprising the continental (Amazon basin) and oceanic (WTNA) portions. Red dots inside the river basin represent in situ flow stations, and the insert area (black rectangle) represents the NECC export water pathway bounded by 55–40°W and 8–9.5°N. This fixed area domain contains the maximum zonal extent of river water and captures the seasonal and interannual SSS variability caused by the Amazon river discharge (Coles et al., 2013; Gouveia et al., 2019). The boxes in the globes relate to the climate indexes of AMO, NTA, and ENM. The latter is calculated using the regions defined by ENM W, C, and E according to Wang et al. (2018). The color gradient in the ocean represents the average SSS (color bar) for September (2002–2017) based on Gouveia et al. (2019).

3. Results and Discussion

3.1. Influence of the Northwest Amazon Basin on the SSS_{NECC}

Negative correlations among precipitation, TWS, river runoff, and SSS_{NECC} are concentrated on the western portion of ARB during the wet season, indicating a significant relation between the decrease in SSS_{NECC} and the increase in precipitation over land (Figures 2a to 2c). This region has low precipitation variance and the highest rainfall of the ARB (~ 3,000 mm/year) (Espinoza et al., 2009; Espinoza et al., 2015), which is counteracted by an evapotranspiration rate of about 1,000 mm/year (Coe et al., 2016). The observed covariation highlights the dominance of this hydrological regime in modulating the interaction of low-salinity water of ARp with the surface ocean. This positive balance of water entering the western portion of ARB every

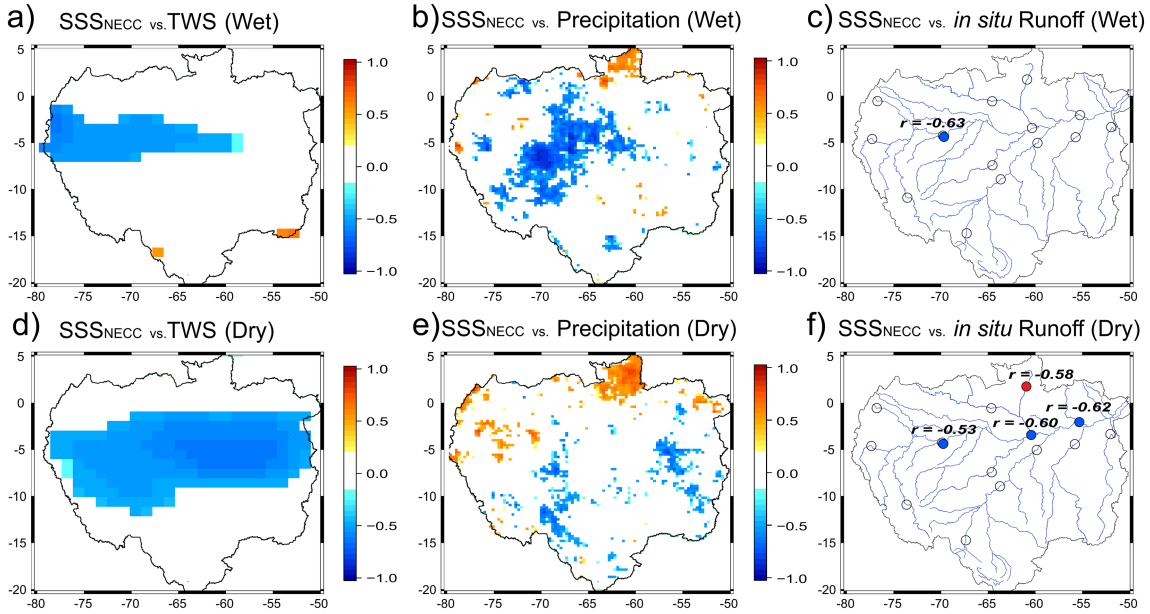

Figure 2. Maps of the ARB showing the pixel-wise correlation of seasonal anomalies (Nov–Apr (wet season) and Jun–Oct (dry season)) of TWS, precipitation, river flow, and the coeval time series of SSS_{NECC} anomalies (calculated from averages inside the black rectangle in Figure 1), for the wet (a–c, respectively) and dry (d–f, respectively) seasons. Only significant correlation values are shown. Red and blue colors indicate positive and negative correlations, respectively. Circles refer to river stations. Light blue lines in Figures 2c and 2f represent the main Amazon tributaries.

year is responsible for about two thirds of the water input to the WTNA (Coe et al., 2016). Based on our results, it is expected that changes in land cover of the western portion of the ARB, which is tightly connected to the ARB water cycle (Aragão, 2012; Spracklen et al., 2012), may cause greater impact on the WTNA water input than changes in other portions of the basin. It should be highlighted that between 2002 and 2018 the ARB has experienced high deforestation rates around 10,333.34 km^2/year (INPE, 2019).

Negative correlations between TWS and SSS_{NECC} dominate the central portion of the ARB during the dry season, becoming stronger toward the east (Figure 2d). The spatial pattern of correlations between precipitation and SSS_{NECC} in the dry season (Figure 2e) is diffuse, possibly because of the complex spatiotemporal distribution of rainfall (Espinoza et al., 2009). Changes in river level during the dry season are known to be caused by anomalies in the seasonal cycle and depend on the rainfall in the previous wet season (Marengo & Espinoza, 2016). The increase in correlation values toward the east (Figures 2d and 2f) is consistent with the proximity to the Amazon delta, where maximum rainfall occurs from March-April-May, known as one of the rainiest regions of the Amazon basin under the direct influence of the ITCZ (Coe et al., 2016; Xie & Carton, 2004). This negative correlation in the dry season may also be partially explained by the time the precipitated water in wet season takes to infiltrate and drain to the Amazon River mouth (Figure 2f). The long residence time of water in the ARB causes the peak flow in the dry season to take 3–6 months to travel between the western and southern tributaries to reach Óbidos station (Foley et al., 2002).

3.2. The SSS_{NECC} as an Indicator of the ARB Hydrological Cycle

Between July and September, the NBC retroflection is most intense and the SSS_{NECC} reaches its lowest values influenced by the Amazon River outflow. This imposes a strong seasonal behavior to the export of most of the plume water (Figure 3a), which is linked to the northernmost position of the ITCZ in September and the northward shift of trade winds that intensifies the NECC (Grodsky & Carton, 2002). The maximum average distance of eastward low-salinity water export, based on a threshold of 35 psu, obtained from SSS_{NECC} values shows a significant ($p < 0.05$) increase from 2009 onward (Figure 3a). This is coincident with the interannual variability of the SSS_{NECC} expressed by a decreasing trend shown in Figures 3b and 3c. Both the increase of eastward ARp water export distance and the decrease of SSS_{NECC} are related to the freshwater input to the NBC retroflection from the western portion of the ARB, with an estimated reduction of the SSS_{NECC} of 0.03 psu/year (~ 3.5%) since 2002. Model experiments (Coles et al.,

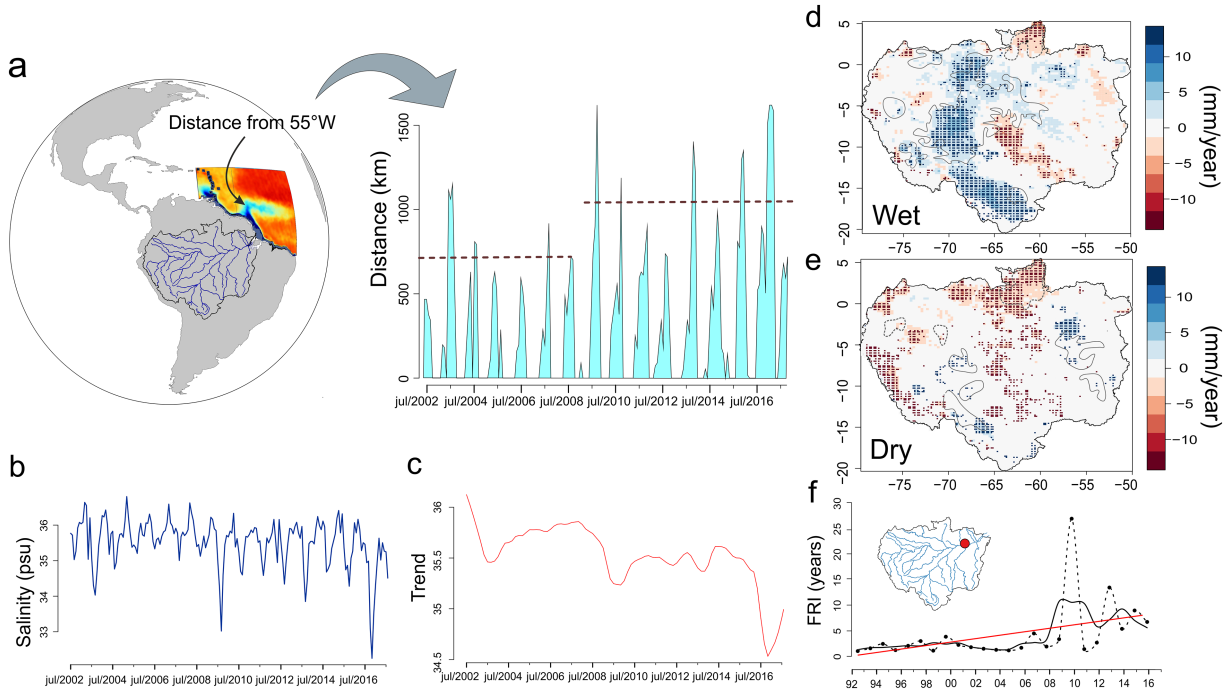

Figure 3. (a) SSS_{NECC} time series (2002–2017) and (b) its temporal trend. (c) Maximum eastward distance traveled by the ARp, measured from 55°W, showing that the maximum annual exports are different between 2002–2008 and 2009–2019 (dashed lines) ($p < 0.05$ for the Mann-Whitney test). The color gradient in the ocean is the same as in Figure 1. Precipitation trends in the ARB for wet (d) and dry seasons (e). All grid cells with significant trends over 90% confidence level are marked with black dots. The gray contours represent the regions of positive (dashed) and negative (continuous) significant correlations between SSS_{NECC} and precipitation. (f) Observed change in flood recurrence between 1992 and 2016 of Óbidos flow station calculated from water level in situ data (dashed line) (the red line fit is the significant (slope error ± 0.07, $p < 0.05$) trend of flood recurrence (Gumbel, 1958) (details in Text S4)). The continuous line represents flood recurrence smoothed with a three points moving average.

2013; Ferry & Reverdin, 2004) suggest that riverine influence on SSS is strongest to the west of longitude 40° W. In fact, cross-correlation analysis found no significant relation between SSS_{NECC} and ocean precipitation over the surrounding oceanic region (Text S3 and Figure S1). The riverine influence on the maximum eastward extension of the SSS_{NECC} is reinforced by weak relationship between SSS and ocean precipitation (Tzortzi et al., 2013) and surface wind velocities (magnitude and zonal component) (Figure S2).

Precipitation over the ARB between 2002 and 2017 presents a significant positive trend during the wet season in two different areas (Figure 3d). One limited between 0 to 10°S and 73°W to 66°W (Solimões and its transition to the Negro sub-basin), and the second between 15 S° to 20°S and 70°W to 61°W (Madeira sub-basin). Areas with positive trends in Figure 3d are coincident with those regions with higher correlation with SSS_{NECC} (see Figure 2b). The dry season precipitation shows a negative trend located in the north and southwest, near the river heads (Figure 3e). Wet season positive precipitation trends agree with increasing flood recurrence at Óbidos between 1992 and 2016; the significant positive trend after 2007 (Figure 3f) coincides with the increase in the maximum average distance of eastward low-salinity water export shown in Figure 3a.

The ENM shows a regime change between 2009 and 2010 with SSTAs becoming more negative from 2009 to 2015/2016, while the NTA and the Atlantic Multidecadal Oscillation present continuous positive trends (Figure 4a). The year of 2009 coincided with a equatorial North Atlantic cooling, which positioned the ITCZ southward of its mean position, causing severe flooding in the Amazon basin and increasing river discharge (Foltz et al., 2012; Grodsky et al., 2014). Our analysis also revealed that these climate indexes significantly explained 98% ($p < 0.05$) of the SSS_{NECC} variability (Figure 4b) reinforcing the idea that the tropical North Atlantic SSTAs and El Niño–Southern Oscillation (ENSO) are the two main mechanisms that influence the interannual variability of precipitation in the ARB (Yoon & Zeng, 2010). A wet/dry dipole over the western/eastern Amazonia has been attributed to the central equatorial Pacific SSTAs related to the

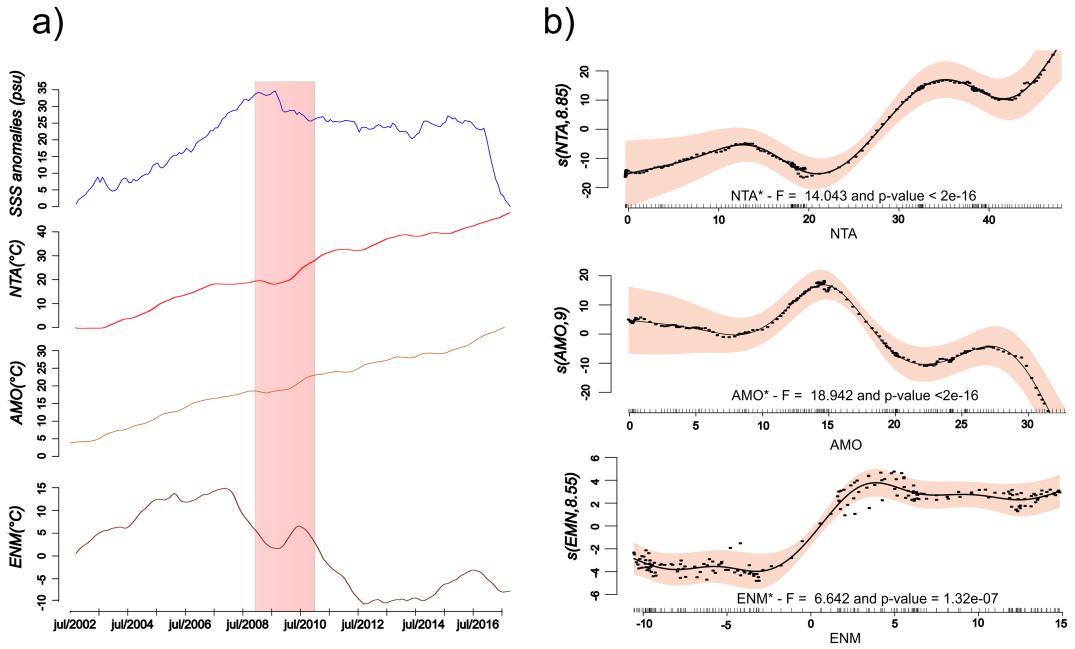

Figure 4. (a) Cumulative sums for SSS_{NECC} anomalies and the climate indexes ENM, NTA, and AMO indicating temporal trends. The red stripe highlights the 2009–2010 transition. (b) Effects of cumulative sums of NTA, ENM, and AMO on the SSS_{NECC} represented by normalized partial residuals. Red fill indicates the 95% confidence interval. The abscissa axes are in logarithmic scale. The *F* tests and their respective *p* values are shown inside each plot.

ENM index (Jiménez-Muñoz et al., 2016). The ENSO associated with the central Pacific SSTAs occurs more frequently when compared to canonical ENSO during the late twentieth century (McPhaden et al., 2011; Yu et al., 2010).

Our results point to a likely ocean-atmosphere-land teleconnection linking the reduction in SSS_{NECC} (Figures 3b and 3c) with an increase in export of ARp water (Figure 3a), ARB precipitation (Figure 3d), and positive SSTAs in the tropical Atlantic (Figure 4) (Vizy & Cook, 2010). This seems to violate the commonly accepted notion of an anticorrelation between interannual variability in the hydrology record and the tropical North Atlantic SSTAs (Giannini et al., 2003; Hastenrath & Greischar, 1993). However, negative rainfall anomalies over the western Amazonia were correlated with the El Niño event of 1972–1973, whereas negative rainfall anomalies over the eastern and central Amazonia and positive anomalies in the west were correlated with the 1982–1983 El Niño (Marengo & Nobre, 2001). In a recent paper, Gloor et al. (2013) suggested that positive SSTAs over the tropical Atlantic and the consequent northward shift of the ITCZ mean position may not be enough to explain Amazon River discharge anomalies. They proposed a process in which positive SST trends in the tropical Atlantic after 1990 increased the landward transport of atmospheric water vapor from the ocean into the Amazon basin by the trade winds, consequently increasing the precipitation rates over the basin (Gloor et al., 2013; Gloor et al., 2015) (exemplified Figures 5a–5c, Text S5, and Figure S3). This positive precipitation feedback would increase in the amount of water fed into the WTNA as seen in at Óbidos station, especially in the wet season [Gloor et al., 2015; see their Figure 1 and our Figure 5d]. The positive trend of SSTAs in the NTA, associated with the decrease in the ENM (Figure 4), is also known to intensify the ARB hydrological cycle (Barichivich et al., 2018). The contrast between SST and sea level pressure between the Atlantic and the Pacific basins contributes to the intensification of the Walker circulation and the deep convection over the ARB (Barichivich et al., 2018).

Based on the above evidences, we hypothesize a conceptual model where the increase of positive SSTAs in the northern tropical Atlantic over the last 16 years caused an increase in latent heat flux for the atmosphere, increasing the amount of moisture over the ocean [see Gloor et al., 2013] (Figure 5a and Figure S3). This process is magnified by the contrast of SSTAs between the Atlantic and the Pacific Oceans (Barichivich et al., 2018), strengthening the trade winds and increasing the moisture transport to the ARB

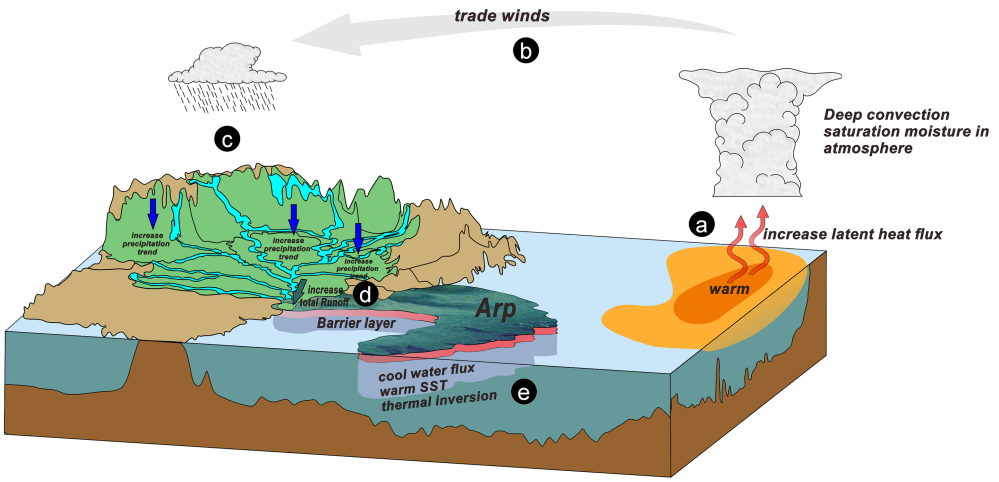

Figure 5. Conceptual model of the impact of ARB hydrological intensification on the WTNA. (a) The increase of latent heat flux for atmosphere induced by warm SSTAs in the Atlantic introduces more moisture to the atmosphere. (b) Excess moisture is advected into the ARB by trade winds leading to (c) increase in precipitation, where blue arrows indicate the areas that present significant trend in Figure 4. The previous processes would lead to (d) more riverine water being discharged into the WTNA, (e) reducing the entrainment of cool water flux and strengthening the formation of a barrier layer.

(Servain et al., 2014) (Figure 5b), contributing to positive precipitation trend in the western portion of Amazon during wet season (Figure 5c). The increase in the NECC export of freshwater can thicken the barrier layer, reduce vertical mixing (Figure 5d), and form a strong pycnocline below the mixed layer (Balaguru et al., 2012). Pailler et al. (1999) showed that a large part of the barrier layer induced by freshwater occurred within the retroflection area of NBC. The thicker barrier layer reduces the mixed layer depth, and this shallow surface layer captures more wind momentum, producing strong surface currents and increasing the eastward export of low-salinity water (Figure 5e) (Coles et al., 2013).

4. Conclusions

We propose, for the first time, a process-oriented model that tries to elucidate how hydrological regime in the western portion of ARB is modulating the interaction of low-salinity water of ARp with SSS_{NECC} variability within the main export pathway of river water into the WTNA. On the ocean side it was also observed an increase in the eastward advection of ARp water concurrent with a decrease of SSS_{NECC}. The reduction of SSS_{NECC} and increase in export of ARp water are closely linked with the ARB precipitation and positive feedbacks associated to SSTAs in the tropical Atlantic. We propose a conceptual model that links ocean, atmosphere, and continental processes responsible for the hydrological cycle intensification.

Acknowledgments
This study was financed in part by the Coordenação de Aperfeiçoamento de Pessoal de Nível Superior - Brasil (CAPES) - Finance Code 001. The German Research Centre for Geosciences, ORE-HYBAM, National Oceanic and Atmospheric Administration, Goddard Earth Sciences Data and Information Services Center, and European Centre for Medium-Range Weather Forecasts are thanked for providing data used in the analyses. Tropical Rainfall Measuring Mission satellite of the TRMM 3B43v7 product is available at https://disc.gsfc.nasa.gov/datasets/TRMM_3B437/summary. Total water storage from the Gravity Recovery and Climate Experiment is available at http://grace.jpl.nasa.gov/data/get-data/. Runoff data of all Amazon sub-basins obtained from the Hydrogeodynamics of the Amazon Basin Observatory is available at http://www.ore-hybam.org/. The Atlantic Multidecadal Oscillation and the North Tropical Atlantic indexes are available at https://www.esrl.noaa.gov/psd/data/climateindices/list/, and the El Niño Modoki at http://www.jamstec.go.jp/frsgc/research/d1/iod/DATA/emi.monthly.txt. Wind data were obtained from https://www.ecmwf.int/en/forecasts/datasets/reanalysis-datasets/era-interim.Surface salinity data used in this paper are available at https://figshare.com/s/e55c10dc78fed648a1ef.

References

Aragão, L. E. O. C. (2012). The rainforests water pump. *Nature*, *489*(7415), 217–218. https://doi.org/10.1038/nature11485

Balaguru, K., Chang, P., Saravanan, R., & Jang, C. J. (2012). The barrier layer of the Atlantic warmpool: Formation mechanism and influence on the mean climate. *Tellus A: Dynamic Meteorology and Oceanography*, *64*(1), 18162. https://doi.org/10.3402/tellusa.v64i0.18162

Barichivich, J., Gloor, E., Peylin, P., Brienen, R. J., Schöngart, J., Espinoza, J. C., & Pattnayak, K. C. (2018). Recent intensification of Amazon flooding extremes driven by strengthened walker circulation. *Science advances*, *4*(9), eaat8785. https://doi.org/10.1126/sciadv.aat8785

Cleveland, R. B., Cleveland, W. S., McRae, J. E., & Terpenning, I. (1990). Stl: A seasonal-trend decomposition. *Journal of official statistics*, *6*(1), 3–73.

Coe, M. T., Macedo, M. N., Brando, P. M., Lefebvre, P., Panday, P., & Silvério, D. (2016). *The hydrology and energy balance of the Amazon basin. In Interactions between biosphere, atmosphere and human land use in the Amazon basin* (pp. 35–53). Berlin, Heidelberg: Springer.

Coles, V. J., Brooks, M. T., Hopkins, J., Stukel, M. R., Yager, P. L., & Hood, R. R. (2013). The pathways and properties of the Amazon River plume in the tropical north Atlantic Ocean. *Journal of Geophysical Research: Oceans*, *118*, 6894–6913. https://doi.org/10.1002/2013JC008981

Dahle, C., Flechtner, F., & Gruber, C. (2012). Gfz grace level-2 processing standards document for level-2 product release 0005. GeoForschungsZentrum Potsdam.

Dai, A., & Trenberth, K. E. (2002). Estimates of freshwater discharge from continents: Latitudinal and seasonal variations. *Journal of Hydrometeorology*, *3*(6), 660–687. https://doi.org/10.1175/1525-7541(2002)003<0660:EOFDFC>2.0.CO;2

Nascimento, M. G., Herdies, D. L., & Oliveira de Souza, D. (2016). The South American water balance: The influence of jets. *Journal of Climate*, *29*(4), 1429–1449. https://doi.org/10.1175/JCLID-15-0065.1

Drumond, A., Marengo, J., Ambrizzi, T., Nieto, R., Moreira, L., & Gimeno, L. (2014). The role of the Amazon basin moisture in the atmospheric branch of the hydrological cycle: A Lagrangian analysis. *Hydrology and Earth System Sciences*, *18*(7), 2577–2598. https://doi.org/10.5194/hess-18-2577-2014

Eltahir, E. A., & Bras, R. L. (1994). Precipitation recycling in the Amazon basin. *Quarterly Journal of the Royal Meteorological Society*, *120*(518), 861–880. https://doi.org/10.1002/qj.49712051806

Enfield, D. B. (1996). Relationships of inter-American rainfall to tropical Atlantic and Pacific SST variability. *Geophysical Research Letters*, *23*(23), 3305–3308. https://doi.org/10.1029/96GL03231

Espinoza, J. C., Chavez, S., Ronchail, J., Junquas, C., Takahashi, K., & Lavado, W. (2015). Rainfall hotspots over the southern tropical Andes: Spatial distribution, rainfall intensity, and relations with large-scale atmospheric circulation. *Water Resources Research*, *51*, 3459–3475. https://doi.org/10.1002/2014WR016273

Espinoza, J. C., Marengo, J. A., Ronchail, J., Carpio, J. M., Flores, L. N., & Guyot, J. L. (2014). The extreme 2014 flood in south-western Amazon basin: The role of tropical-subtropical south Atlantic SST gradient. *Environmental Research Letters*, *9*(12). https://doi.org/10.1088/1748-9326/9/12/124007

Espinoza, J. C., Ronchail, J., Guyot, J. L., Cochonneau, G., Naziano, F., Lavado, W., & Vauchel, P. (2009). Spatio-temporal rainfall variability in the Amazon basin countries (Brazil, Peru, Bolivia, Colombia, and Ecuador). *International Journal of Climatology: A Journal of the Royal Meteorological Society*, *29*(11), 1574–1594. https://doi.org/10.1002/joc.1791

Ferry, N., & Reverdin, G. (2004). Sea surface salinity interannual variability in the western tropical Atlantic: An ocean general circulation model study. *Journal of Geophysical Research*, *109*, C05026. https://doi.org/10.1029/2003JC002122

Field, A. (2007). Amazon and Orinoco river plumes and NBC rings: Bystanders or participants in hurricane events? *Journal of climate*, *20*(2), 316–333. https://doi.org/10.1175/JCLI3985.1

Foley, J. A., Botta, A., Coe, M. T., & Costa, M. H. (2002). El Niño–Southern Oscillation and the climate, ecosystems and rivers of Amazonia. *Global Biogeochemical Cycles*, *16*(4), 1132. https://doi.org/10.1029/2002GB001872

Foltz, G. R., & McPhaden, M. J. (2008). Seasonal mixed layer salinity balance of the tropical north Atlantic Ocean. *Journal of Geophysical Research*, *113*, C02013. https://doi.org/10.1029/2007JC004178

Foltz, G. R., McPhaden, M. J., & Lumpkin, R. (2012). A strong Atlantic meridional mode event in 2009: The role of mixed layer dynamics. *Journal of Climate*, *25*(1), 363–380. https://doi.org/10.1175/JCLI-D-11-00150.1

Fournier, S., Vandemark, D., Gaultier, L., Lee, T., Jonsson, B., & Gierach, M. (2017). Interannual variation in offshore advection of Amazon-Orinoco plume waters: Observations, forcing mechanisms, and impacts. *Journal of Geophysical Research: Oceans*, *122*, 8966–8982. https://doi.org/10.1002/2017JC013103

Giannini, A., Saravanan, R., & Chang, P. (2003). Oceanic forcing of Sahel rainfall on interannual to interdecadal time scales. *Science*, *302*(5647), 1027–1030. https://doi.org/10.1126/science.1089357

Gloor, M., Barichivich, J., Ziv, G., Brienen, R., Schöngart, J., Peylin, P., et al. (2015). Recent Amazon climate as background for possible ongoing and future changes of Amazon humid forests. *Global Biogeochemical Cycles*, *29*, 1384–1399. https://doi.org/10.1002/2014GB005080

Gloor, M., Brienen, R. J., Galbraith, D., Feldpausch, T., Schongart, J., Guyot, J.-L., & Phillips, O. (2013). Intensification of the Amazon hydrological cycle over the last two decades. *Geophysical Research Letters*, *40*, 1729–1733. https://doi.org/10.1002/grl.50377

Gouveia, N., Gherardi, D., Wagner, F., Paes, E., Coles, V., & Aragão, L. (2019). The salinity structure of the Amazon River plume drives spatiotemporal variation of oceanic primary productivity. *Journal of Geophysical Research: Biogeosciences*, *124*, 147–165. https://doi.org/10.1029/2018JG004665

Grodsky, S. A., & Carton, J. A. (2002). Surface drifter pathways originating in the equatorial Atlantic cold tongue. *Geophysical Research Letters*, *29*(23), 2147. https://doi.org/10.1029/2002GL015788

Grodsky, S. A., Reverdin, G., Carton, J. A., & Coles, V. J. (2014). Year-to-year salinity changes in the Amazon plume: Contrasting 2011 and 2012 Aquarius/SACD and SMOS satellite data. *Remote Sensing of Environment*, *140*, 14–22. https://doi.org/10.1016/j.rse.2013.08.033

Gumbel, E. J. (1958). *Statistics of extremes*. New York: Columbia University Press.

Hastenrath, S., & Greischar, L. (1993). Circulation mechanisms related to northeast Brazil rainfall anomalies. *Journal of Geophysical Research*, *98*(D3), 5093–5102. https://doi.org/10.1029/92JD02646

Hu, C., Montgomery, E. T., Schmitt, R. W., & Muller-Karger, F. E. (2004). The dispersal of the Amazon and Orinoco river water in the tropical Atlantic and Caribbean Sea: Observation from space and s-palace floats. *Deep Sea Research Part II: Topical Studies in Oceanography*, *51*(10-11), 1151–1171. https://doi.org/10.1016/j.dsr2.2004.04.001

Huffman, G. J., Adler, R. F., Bolvin, D. T., & Nelkin, E. J. (2010). *The TRMM Multi-Satellite Precipitation Analysis (TMPA). In Satellite rainfall applications for surface hydrology* (pp. 3–22). Springer.

Huffman, G. J., Bolvin, D. T., Nelkin, E. J., Wolff, D. B., Adler, R. F., Gu, G., & Stocker, E. F. (2007). The TRMM Multisatellite Precipitation Analysis (TMPA): Quasi-global, multiyear, combined-sensor precipitation estimates at fine scales. *Journal of hydrometeorology*, *8*(1), 38–55. https://doi.org/10.1175/JHM560.1

INPE (2019). Monitoramento da Floresta Amazônica Brasileira por Satélite, Projeto PRODES. Instituto Nacional de Pesquisas Espaciais, São Paulo, Brazil. Available from: http://www.obt.inpe.br/prodes/dashboard/prodes-rates.html (accessed February 2019).

Jiménez-Muñoz, J. C., Mattar, C., Barichivich, J., Santamaría-Artigas, A., Takahashi, K., Malhi, Y., & Van Der Schrier, G. (2016). Record-breaking warming and extreme drought in the Amazon rainforest during the course of El Niño 2015–2016. *Scientific Reports*, *6*, 33130. https://doi.org/10.1038/srep33130

Korosov, A., Counillon, F., & Johannessen, J. A. (2015). Monitoring the spreading of the Amazon freshwater plume by MODIS, SMOS, AQUARIUS, and TOPAZ. *Journal of Geophysical Research: Oceans*, *120*, 268–283. https://doi.org/10.1002/2014JC010155

Lentz, S. J., & Limeburner, R. (1995). The Amazon River plume during AMASSEDS: Subtidal current variability and the importance of wind forcing. *Journal of Geophysical Research*, *100*(C2), 2377–2390. https://doi.org/10.1029/94JC00343

Li, L., Schmitt, R. W., Ummenhofer, C. C., & Karnauskas, K. B. (2016). Implications of North Atlantic sea surface salinity for summer precipitation over the US Midwest: Mechanisms and predictive value. *Journal of Climate*, *29*(9), 3143–3159.

Marengo, J. (2005). The characteristics and variability of the atmospheric water balance in the Amazon basin: Spatial and temporal variability. *Climate Dynamics*, *24*, 11–22.

Marengo, J. (2006). On the hydrological cycle of the Amazon basin: A historical review and current state-of-the-art. *Revista Brasileira de Meteorologia*, *21*(3), 1–19.

Marengo, J., Nobre, C., Tomasella, J., Cardoso, M., & Oyama, M. (2008). Hydroclimatic and ecological behaviour of the drought of Amazonia in 2005. *Philosophical Transactions of the Royal Society of London B: Biological Sciences*, *363*(1498), 1773–1778. https://doi.org/10.1098/rstb.2007.0015

Marengo, J. A., & Espinoza, J. (2016). Extreme seasonal droughts and floods in Amazonia: Causes, trends and impacts. *International Journal of Climatology*, *36*(3), 1033–1050. https://doi.org/10.1002/joc.4420

Marengo, J. A., & Nobre, C. A. (2001). General characteristics and variability of climate in the Amazon basin and its links to the global climate system. In M. E. McClain, R. L. Victoria, & J. E. Richey (Eds.), *The biogeochemistry of the Amazon basin* (pp. 17–41). Oxford: Oxford University Press.

Marengo, J. A., Tomasella, J., Alves, L. M., Soares, W. R., & Rodriguez, D. A. (2011). The drought of 2010 in the context of historical droughts in the Amazon region. *Geophysical Research Letters*, *38*, L12703. https://doi.org/10.1029/2011GL047436

Masson, S., & Delecluse, P. (2001). Influence of the Amazon River runoff on the tropical Atlantic. *Physics and Chemistry of the Earth, Part B: Hydrology, Oceans and Atmosphere*, *26*(2), 137–142. https://doi.org/10.1016/S1464-1909(00)00230-6

McPhaden, M., Lee, T., & McClurg, D. (2011). El Niño and its relationship to changing background conditions in the tropical Pacific Ocean. *Geophysical Research Letters*, *38*, L15709. https://doi.org/10.1029/2011GL048275

Medeiros, P. M., Seidel, M., Ward, N. D., Carpenter, E. J., Gomes, H. R., Niggemann, J., & Dittmar, T. (2015). Fate of the Amazon River dissolved organic matter in the tropical Atlantic Ocean. *Global Biogeochemical Cycles*, *29*, 677–690. https://doi.org/10.1002/2015GB005115

Muller-Karger, F. E., McClain, C. R., & Richardson, P. L. (1988). The dispersal of the Amazon's water. *Nature*, *333*(6168), 56.

Pailler, K., Bourlés, B., & Gouriou, Y. (1999). The barrier layer in the western tropical Atlantic Ocean. *Geophysical Research Letters*, *26*(14), 2069–2072.

Salisbury, J., Vandemark, D., Campbell, J., Hunt, C., Wisser, D., Reul, N., & Chapron, B. (2011). Spatial and temporal coherence between Amazon River discharge, salinity, and light absorption by colored organic carbon in western tropical Atlantic surface waters. *Journal of Geophysical Research*, *116*, C00H02. https://doi.org/10.1029/2011JC006989

Servain, J., Caniaux, G., Kouadio, Y. K., McPhaden, M. J., & Araujo, M. (2014). Recent climatic trends in the tropical Atlantic. *Climate Dynamics*, *43*(11), 3071–3089.

Sorí, R., Marengo, J. A., Nieto, R., Drumond, A., & Gimeno, L. (2018). The atmospheric branch of the hydrological cycle over the Negro and Madeira River basins in the Amazon region. *Water*, *10*(6). https://doi.org/10.3390/w10060738

Spracklen, D. V., Arnold, S. R., & Taylor, C. (2012). Observations of increased tropical rainfall preceded by air passage over forests. *Nature*, *489*(7415), 282.

Stukel, M., Coles, V., Brooks, M., & Hood, R. (2014). Top-down, bottom-up and physical controls on diatom-diazotroph assemblage growth in the Amazon river plume. *Biogeosciences*, *11*(12). https://doi.org/10.5194/bg-11-3259-2014

Subramaniam, A., Yager, P. L., Carpenter, E. J., Mahaffey, C., Björkman, K., Cooley, S., et al. (2008). Amazon River enhances diazotrophy and carbon sequestration in the tropical north Atlantic Ocean. *Proceedings of the National Academy of Sciences*, *105*(30), 10460–10465. https://doi.org/10.1073/pnas.0710279105

Tzortzi, E., Josey, S. A., Srokosz, M., & Gommenginger, C. (2013). Tropical Atlantic salinity variability: New insights from SMOS. *Geophysical Research Letters*, *40*, 2143–2147. https://doi.org/10.1002/grl.50225

Vizy, E. K., & Cook, K. H. (2010). Influence of the Amazon/Orinoco plume on the summertime Atlantic climate. *Journal of Geophysical Research*, *115*, D21112. https://doi.org/10.1029/2010JD014049

Wang, X., Tan, W., & Wang, C. (2018). A new index for identifying different types of El Niño Modoki events. *Climate Dynamics*, *50*(7-8), 2753–2765. https://doi.org/10.1007/s00382-017-3769-8

Xie, S.-P., & Carton, J. A. (2004). Tropical Atlantic variability: Patterns, mechanisms, and impacts. Earth Climate: The Ocean-Atmosphere Interaction. *Geophysical Monograph*, *147*, 121–142.

Yoon, J.-H., & Zeng, N. (2010). An Atlantic influence on Amazon rainfall. *Climate Dynamics*, *34*(2-3), 249–264. https://doi.org/10.1007/s00382-009-0551-6

Yu, J.-Y., Kao, H.-Y., & Lee, T. (2010). Subtropics-related interannual sea surface temperature variability in the central equatorial Pacific. *Journal of Climate*, *23*(11), 2869–2884. https://doi.org/10.1175/2010JCLI3171.1

Zeng, N., Yoon, J.-H., Marengo, J. A., Subramaniam, A., Nobre, C. A., Mariotti, A., & Neelin, J. D. (2008). Causes and impacts of the 2005 Amazon drought. *Environmental Research Letters*, *3*(1). https://doi.org/10.1088/1748-9326/3/1/014002